



The University of Vermont



Role of Elasto-Inertial Turbulence in Polymer Drag Reduction

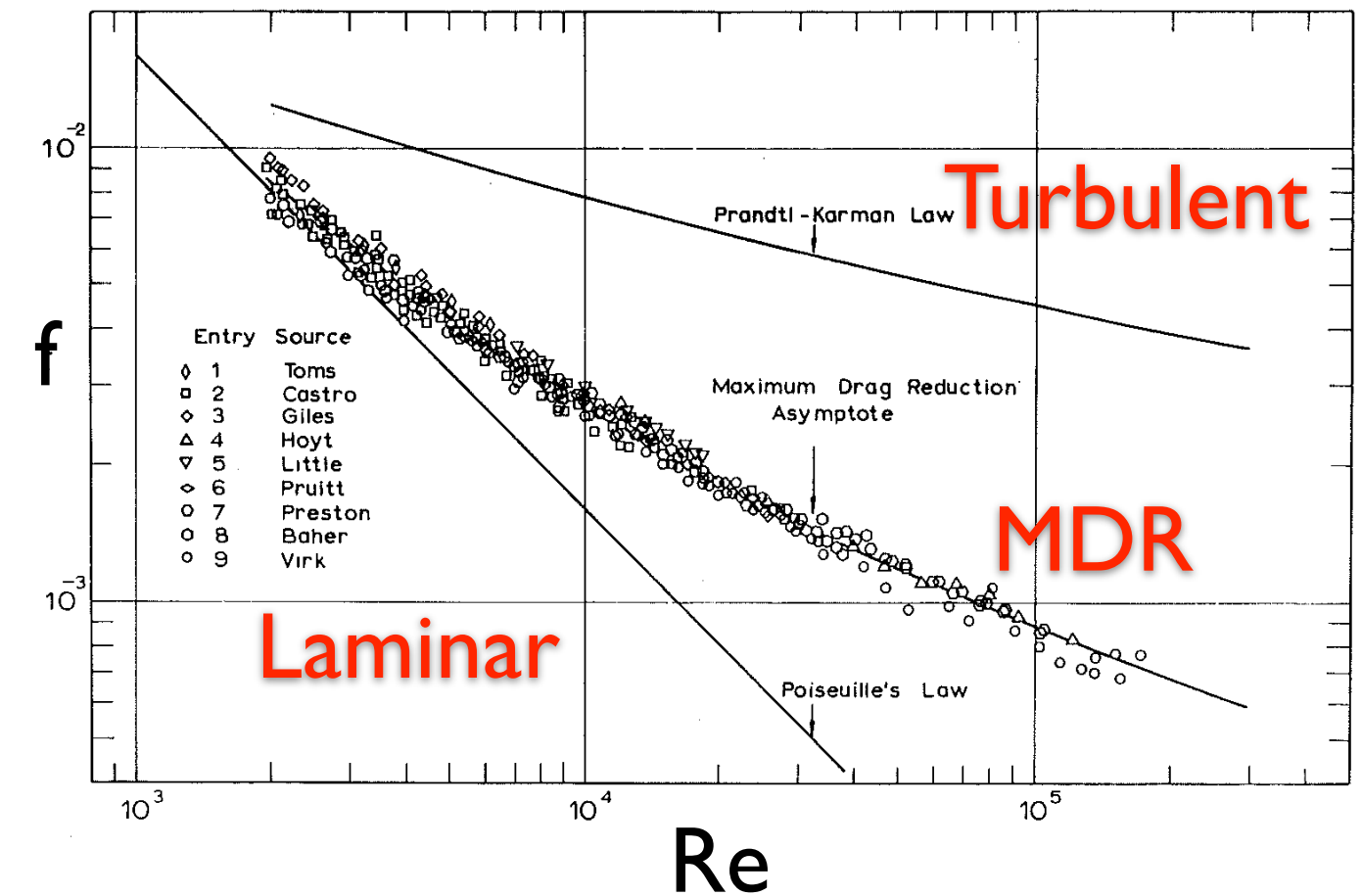
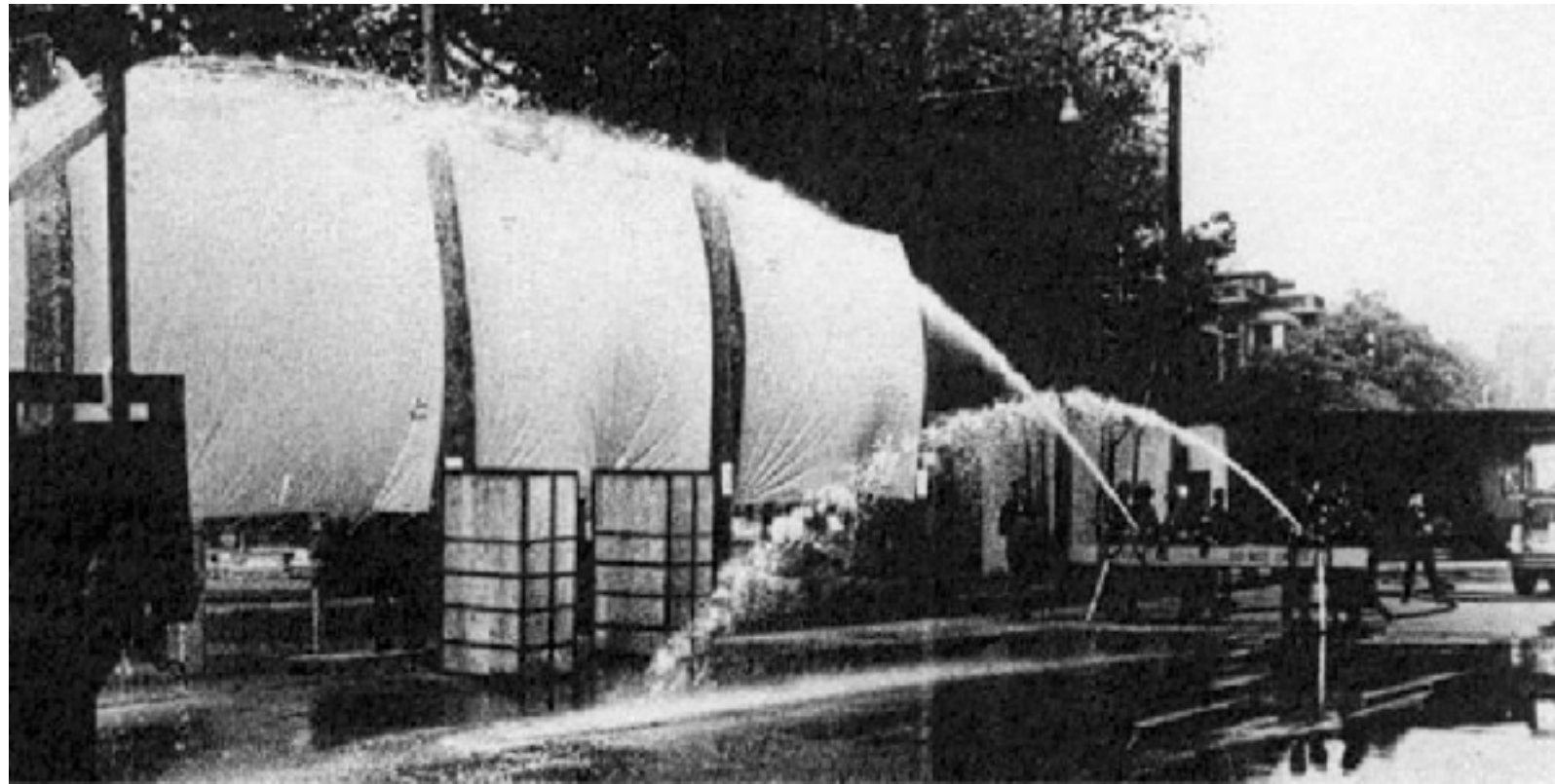
Yves Dubief¹,
Samir Sid², Vincent Terrapon²

1- Department of Engineering, University of Vermont

2- Dept. of Aero. and Mech. Engineering, University of Liege, Belgium

Denver, APS-DFD 2017

Polymer Drag Reduction



- Minute addition of polymers can result in significant reduction of friction drag
- Drag reduction has an upper limit: Maximum Drag Reduction (MDR)

Open Questions

1. What is the nature of MDR?
 - Is it Newtonian (Graham 2004, Procaccia et al. 2008)?
 - Is it EIT, Elasto-Inertial Turbulence (Samantha, 2012; Dubief et al., 2013, Terrapon et al, 2014)?
2. What is the mechanism of EIT?
3. What is the relation between EIT and elastic turbulence?

Motivation

We seek to define the nature of MDR through rigorous numerical experiments and verification.

Assumption 1 (Graham 2014, Procaccia et al. 2008):

- MDR's dynamics intermittently alternates between a laminar edge state and a weak turbulent state driven by Newtonian coherent structures
- MDR's velocity profile is logarithmic

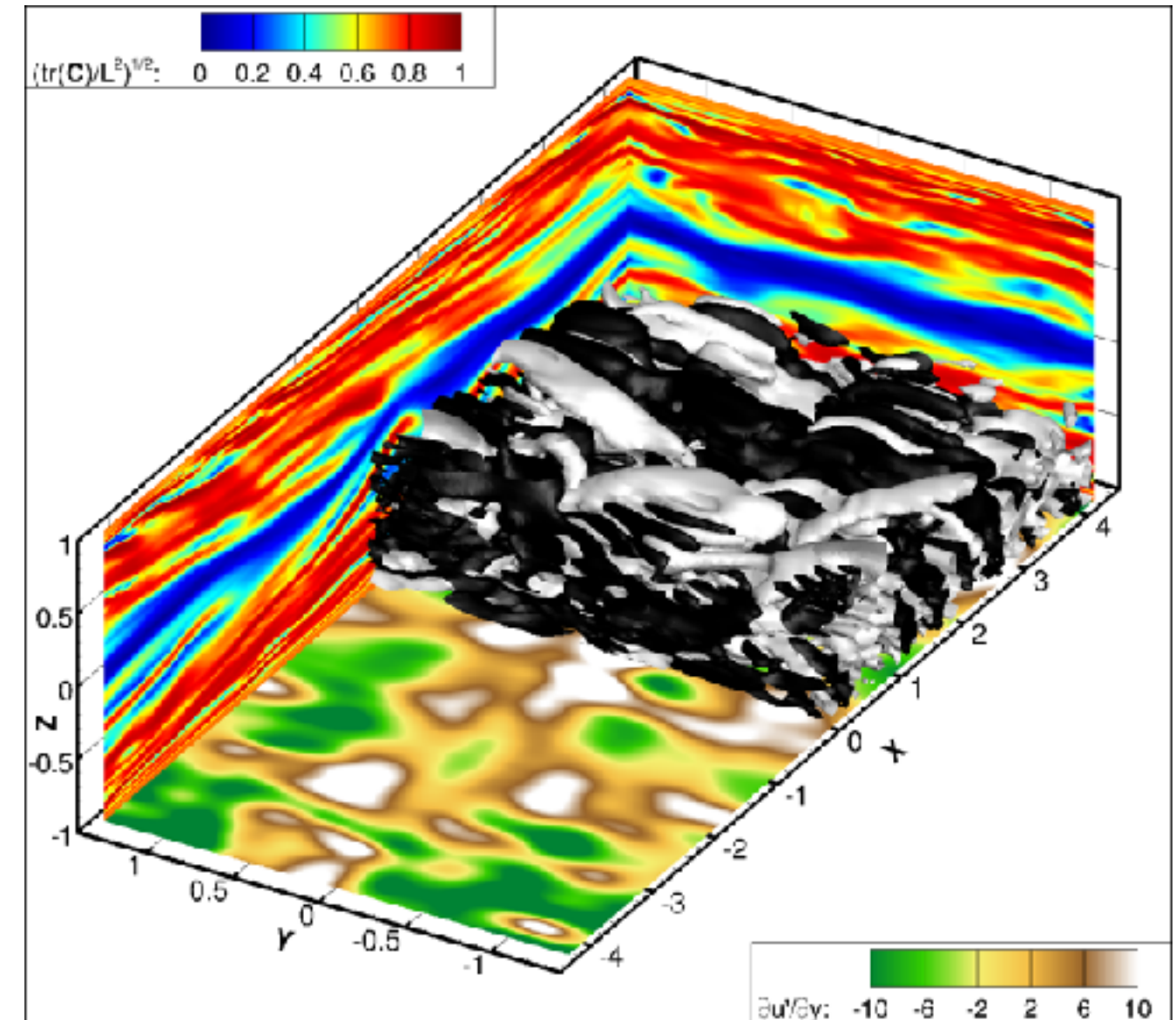
Assumption 2 (Samanta et al. 2013, Dubief et al. 2013, Terrapon et al 2014, Sid et al, 2017)

- MDR is EIT

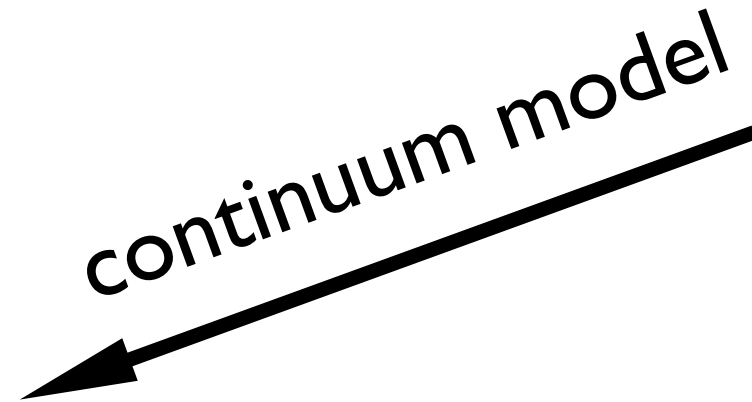
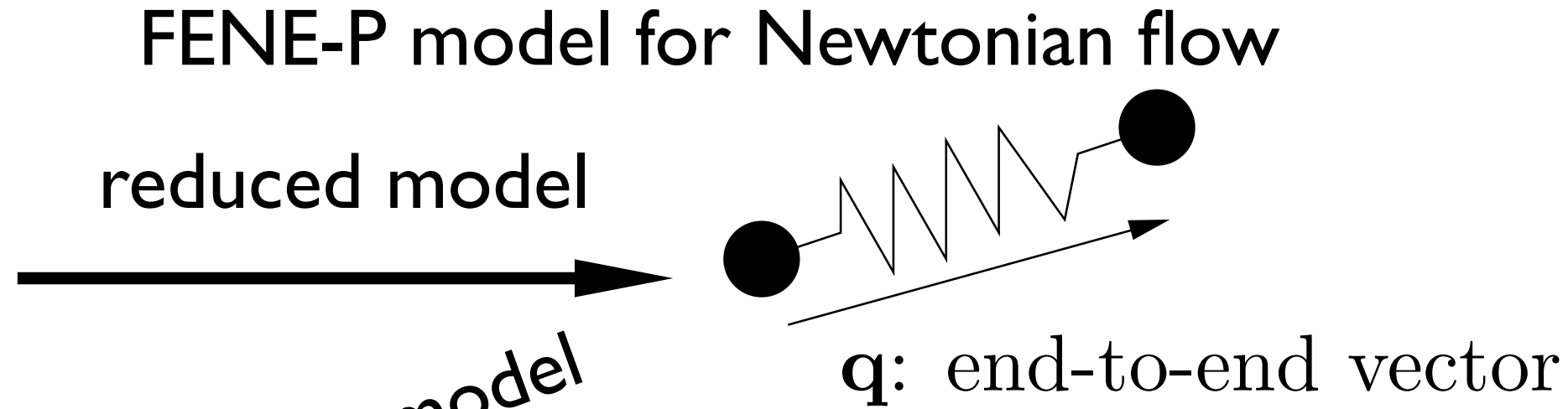
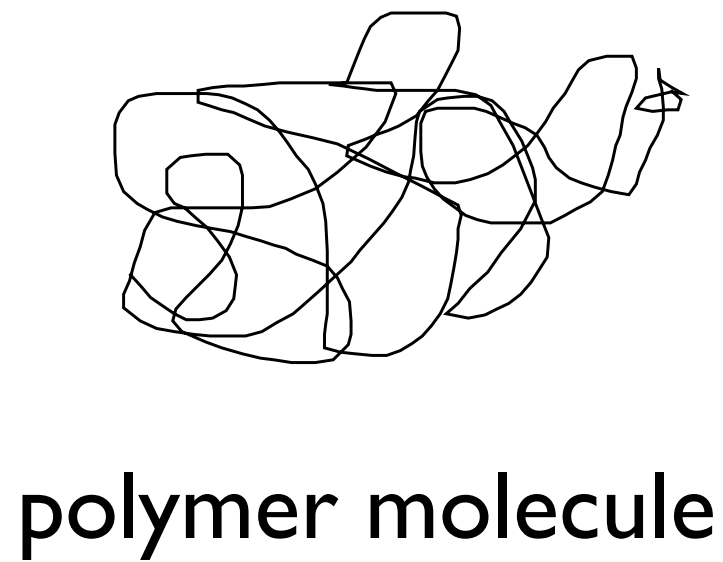
Fact: MDR's velocity profile is not logarithmic (White et al. 2012, Elbing et al. 2013)

Method

- Constant pressure-gradient channel flow simulation
- FENE-P viscoelastic model
- Numerical experiment consists of 3D and 2D minimal channel flow units with controlled diffusion of small-scale polymer dynamics



Viscoelastic Flow Model



Polymer solution parameter

$$\mathbf{C} = C_{ij} = \mathbf{q} \otimes \mathbf{q} = q_i q_j \quad \beta = \frac{\text{solvent viscosity}}{\text{zero-shear polymer solution viscosity}}$$

L : Polymer maximum extension

$$Wi_\tau = \frac{\text{polymer relaxation time}}{\text{viscous flow time scale}} = \frac{\lambda u_\tau^2}{\nu} = \lambda \dot{\gamma}$$

Governing Equations

- Flow field equations

$$\partial_t u_i + \partial_j u_i u_j = -\partial_i p + \frac{1-\beta}{Re} \partial_j \partial_j u_i + \frac{\beta}{Re} \partial_j T_{ij}$$
$$\partial_i u_i = 0$$

- Polymer field equations

$$\partial_t C_{ij} + u_k \partial_k C_{ij} = C_{ik} \partial_k u_j + \partial_k u_i C_{kj} - T_{ij} + \frac{1}{Re Sc} \partial_k \partial_k C_{ij}$$

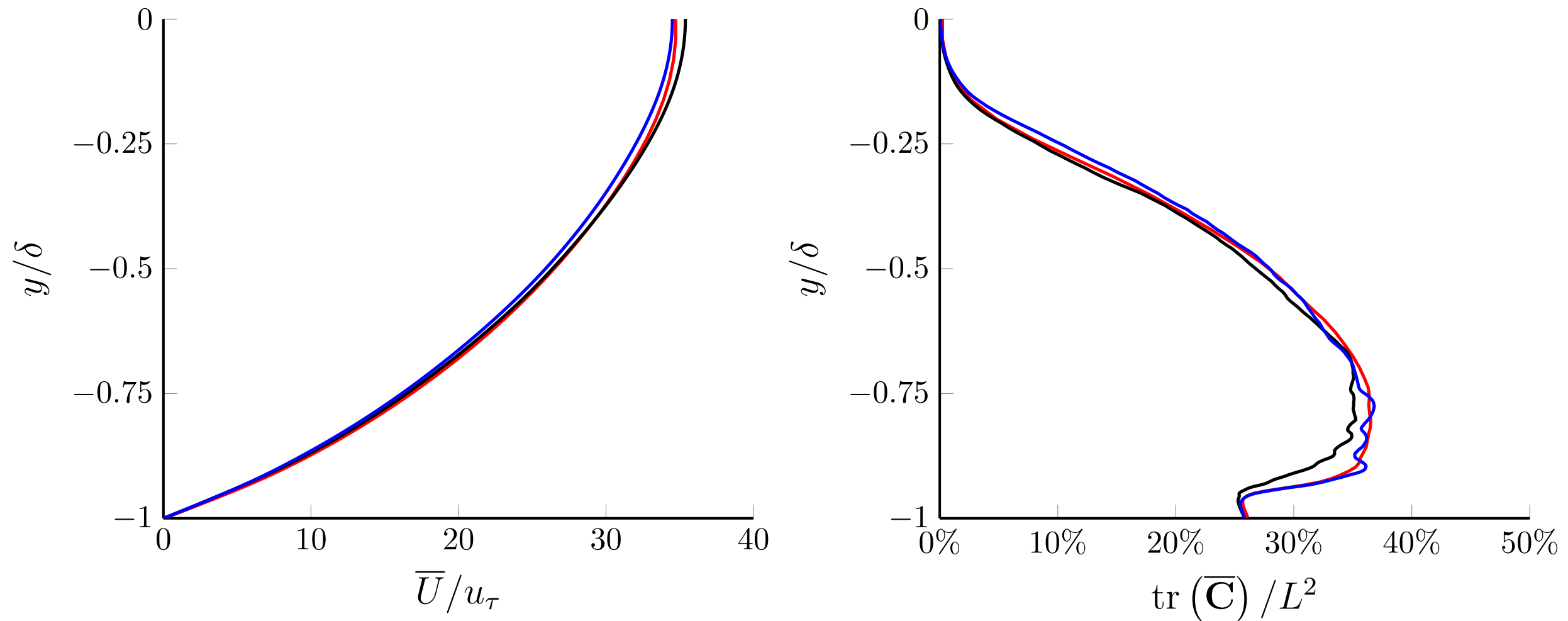
$$T_{ij} = \frac{1}{Wi} \left(\frac{C_{ij}}{1 - C_{kk}/L^2} - \delta_{ij} \right)$$

Numerical Methods

- Code 1: (Dubief et al. 2004, 2005, 2013)
 - Non-dissipative, energy conserving, $\mathcal{O}(\Delta t^2, \Delta x^2)$ finite difference flow solver
 - Polymer advection: $\mathcal{O}(\Delta x^3)$ compact upwind with local artificial dissipation
- Code 2: (Sid et al, 2017)
 - Non-dissipative, energy conserving, $\mathcal{O}(\Delta t^2, \Delta x^2)$ finite volume flow solver
 - Polymer advection: 3rd or 5th order WENO scheme

Verification (Sid et al, 2017)

- Comparison Code 1 (red) and 2 (low res. black, high res. blue)



$$Re_\tau = 84.96, \beta = 0.97, L = 70.7, Wi_\tau = 40$$

Numerical Experiment: Background

$$\partial_t u_i + \partial_j u_i u_j = \partial_i p + \frac{\beta}{Re} \partial_j \partial_j u_i + \frac{1-\beta}{Re} \partial_j T_{ij}$$

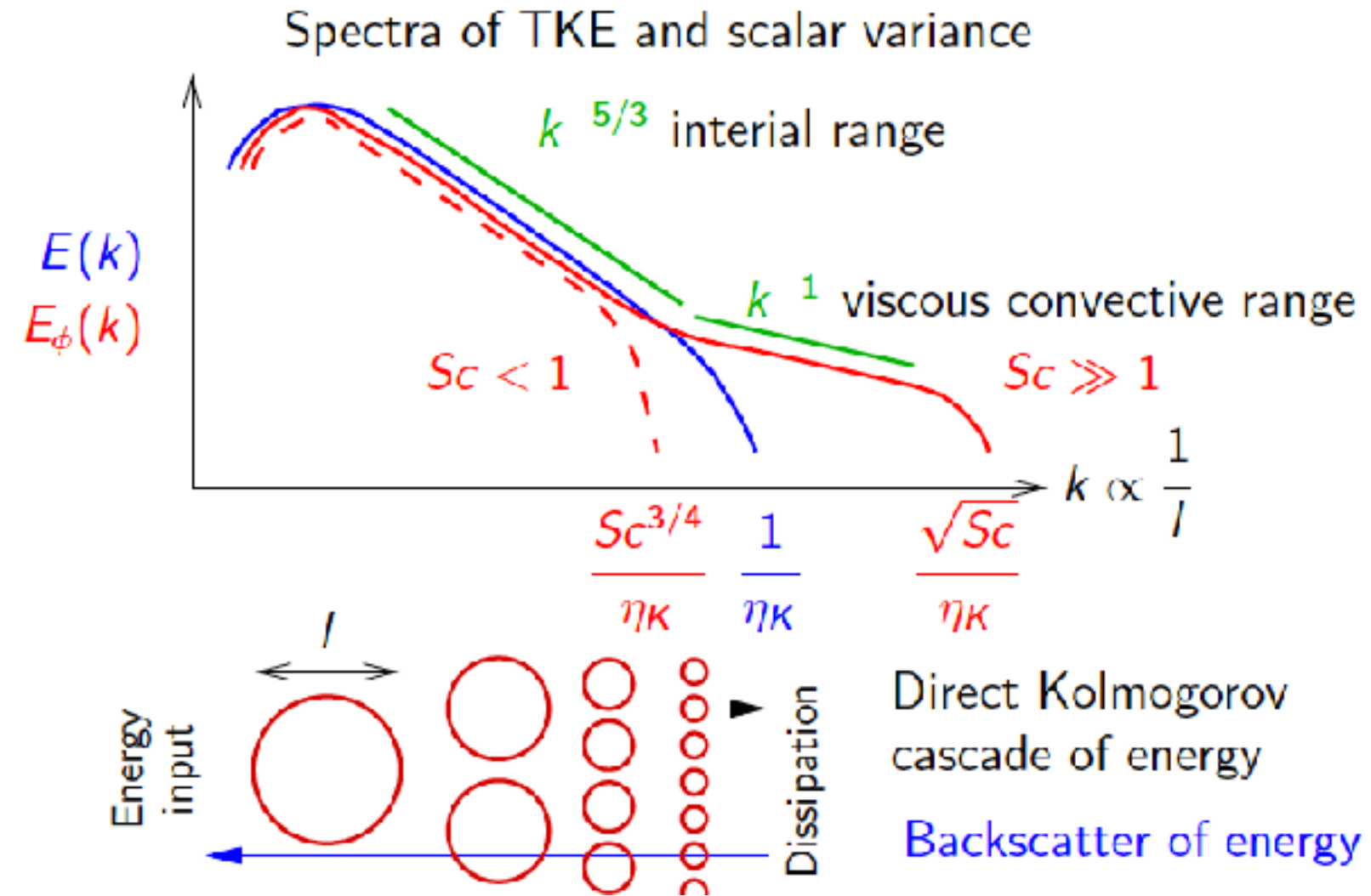
$$\partial_i u_i = 0$$

$$\partial_t C_{ij} + u_k \partial_k C_{ij} = C_{ik} \partial_k u_j + C_{kj} \partial_k u_i - T_{ij} + \frac{1}{Re Sc} \partial_k \partial_k C_{ij}$$

$$T_{ij} = \frac{1}{We} \left(\frac{C_{ij}}{1 - C_{kk}/L^2} - \delta_{ij} \right)$$

- In theory, $Sc = \infty$
- Most polymer simulations use spectral methods, grid resolution same as for Newtonian flow and $Sc \leq 0.5$
- Our simulations use much finer grid resolution and $Sc \gg 1$

Why does Schmidt Matter? Because Batchelor 1959



The left hand side of the theoretical FENE-P model carries no diffusive process and operates on larger time- and length scales than advection (Dubief et al. 2005)

Grounds for Assumption I (MDR=Newtonian)

step size is determined from the CFL stability condition: for the simulations reported in this study, since the spatial grid spacing is fixed, a constant time step $\delta t = 0.02$ is used. An artificial diffusivity term $1/(Sc Re)\nabla^2\alpha$ with $Sc = 0.5$ is added to the FENE-P equation to improve its numerical stability; this magnitude of artificial diffusivity is no larger than most other studies and should not affect the physical interpretation of the results (Sureshkumar & Beris 1997; Ptasinski *et al.* 2003; Housiadas *et al.* 2005; Li *et al.* 2006a; Kim *et al.* 2007). The detailed numerical algorithm used in this study is documented in Xi (2009). The computer code used in this study is based on the Newtonian DNS code *ChannelFlow* written by Gibson (2009).

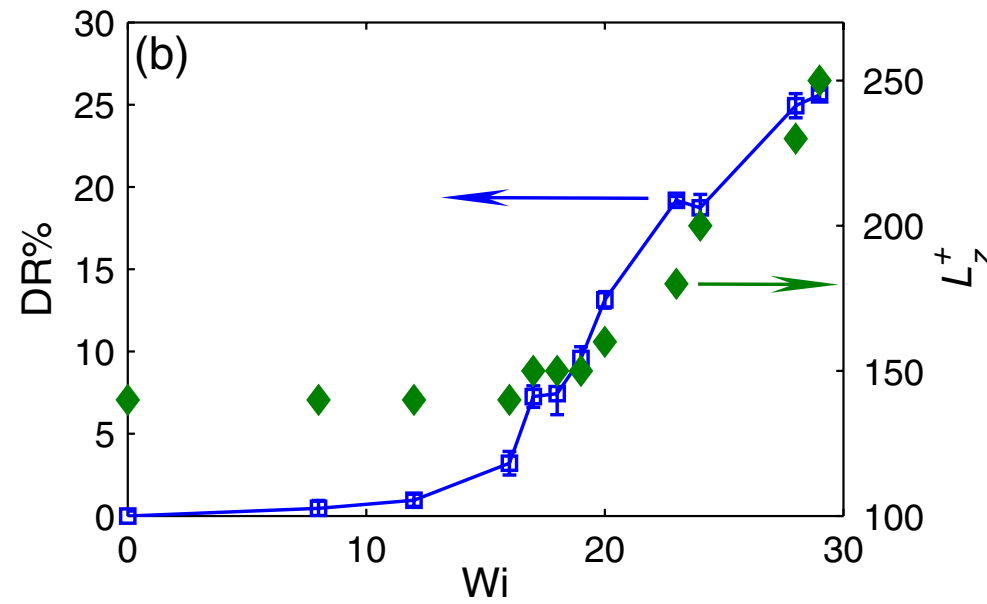


FIG. 2 (color online). (a) Time scales and fraction of time spent in hibernation (b) level of drag reduction and spanwise box size, vs Wi . (At the relatively low Reynolds number considered here, the flow laminarizes for $Wi \gtrsim 31$).

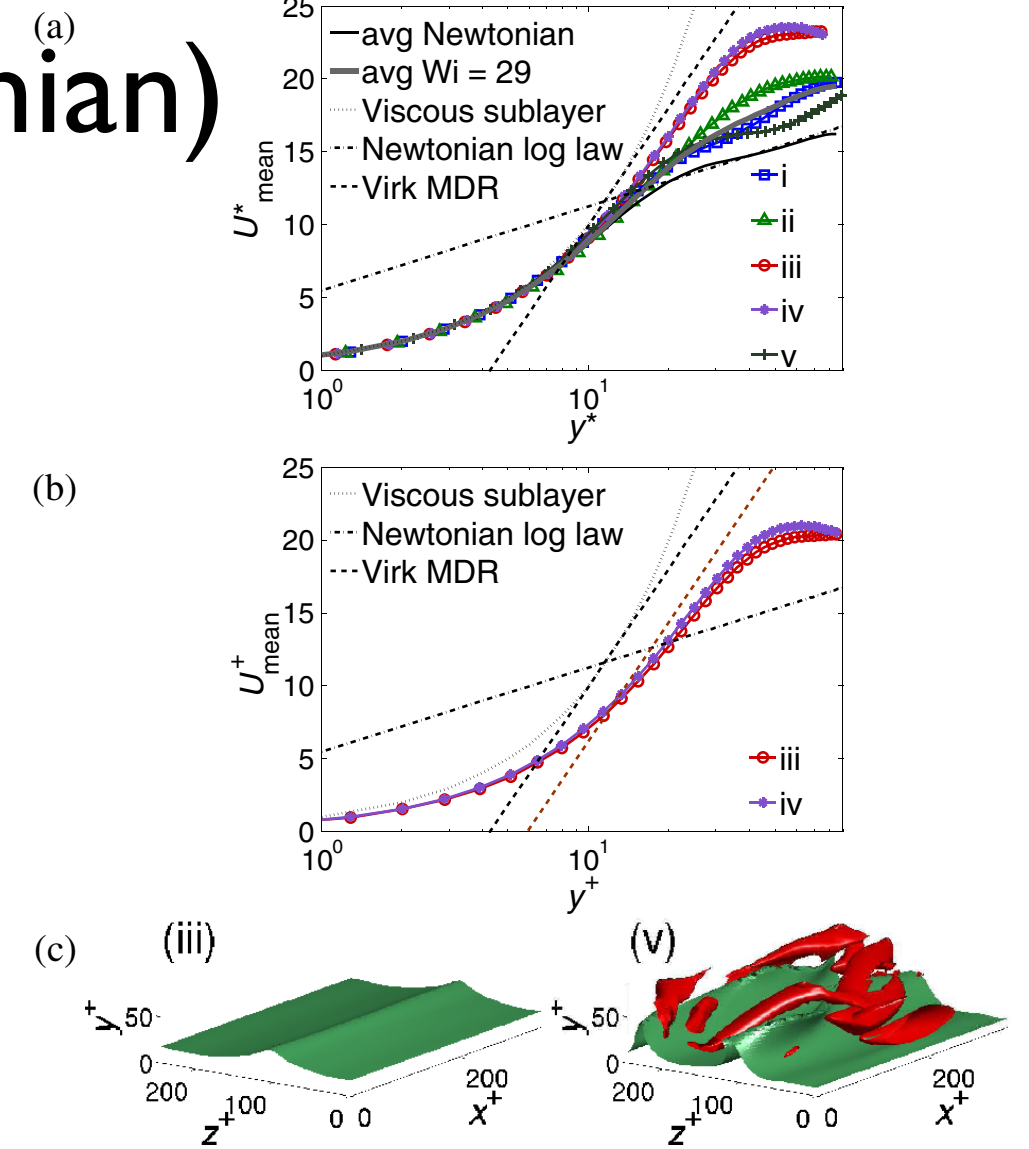
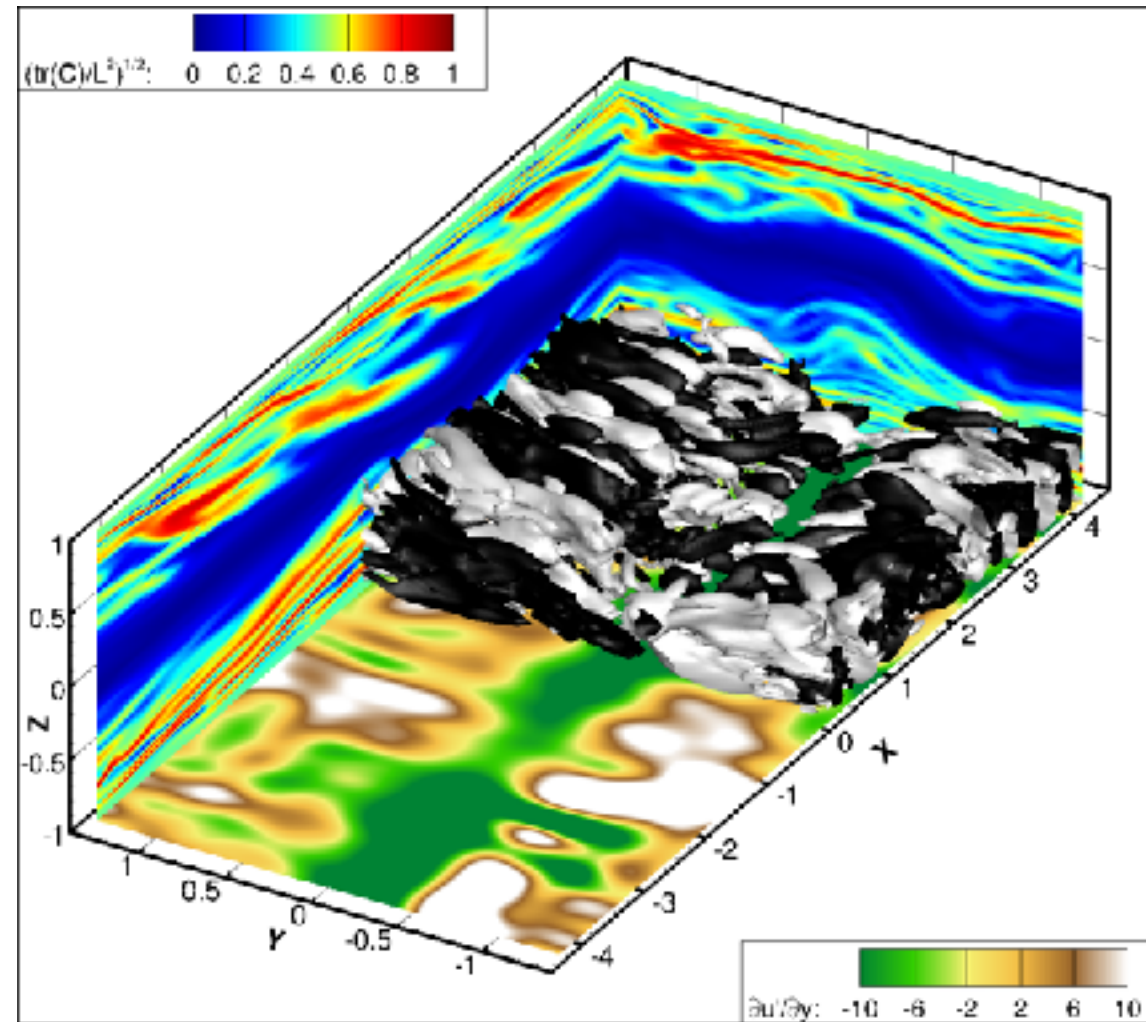


FIG. 4 (color online). (a) Instantaneous mean velocity profiles of snapshots i–v [lighter (colored) lines], and time-averaged profiles in the Newtonian and $Wi = 29$ cases. (The latter are plotted in terms of conventional wall units.) (b) Instantaneous mean velocity profiles from time instants iii and iv plotted in conventional wall units. For comparison, a downward-shifted plot of the Virk log law is also shown. (c) Flow structures of typical snapshots in hibernation (iii) and active turbulence (v). Green sheets are isosurfaces $v_x = 0.3$; pleats correspond to low-speed streaks; red tubes are isosurfaces of streamwise-vortex intensity $Q_{2D} = 0.02$, calculated by applying the Q criterion of vortex identification [25] in the yz plane [5,17].

Grounds for Assumption II (MDR=EIT)

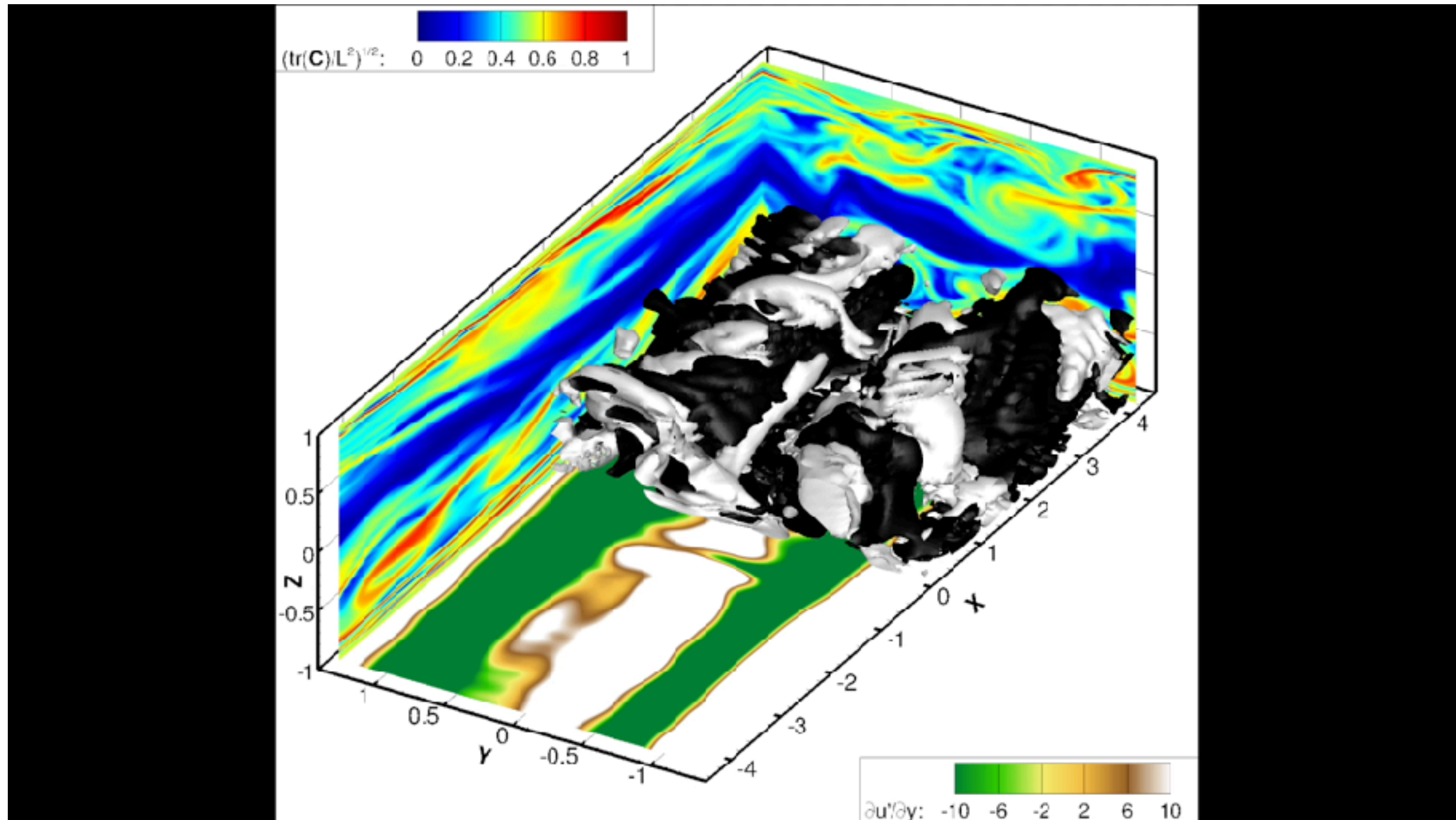
$$Re_\tau = 84.96, \beta = 0.97, L = 70.7, Wi_\tau = 40$$



- Simulation for the same parameters, flow domain as previous slide
- Iso contours of positive and negative Q

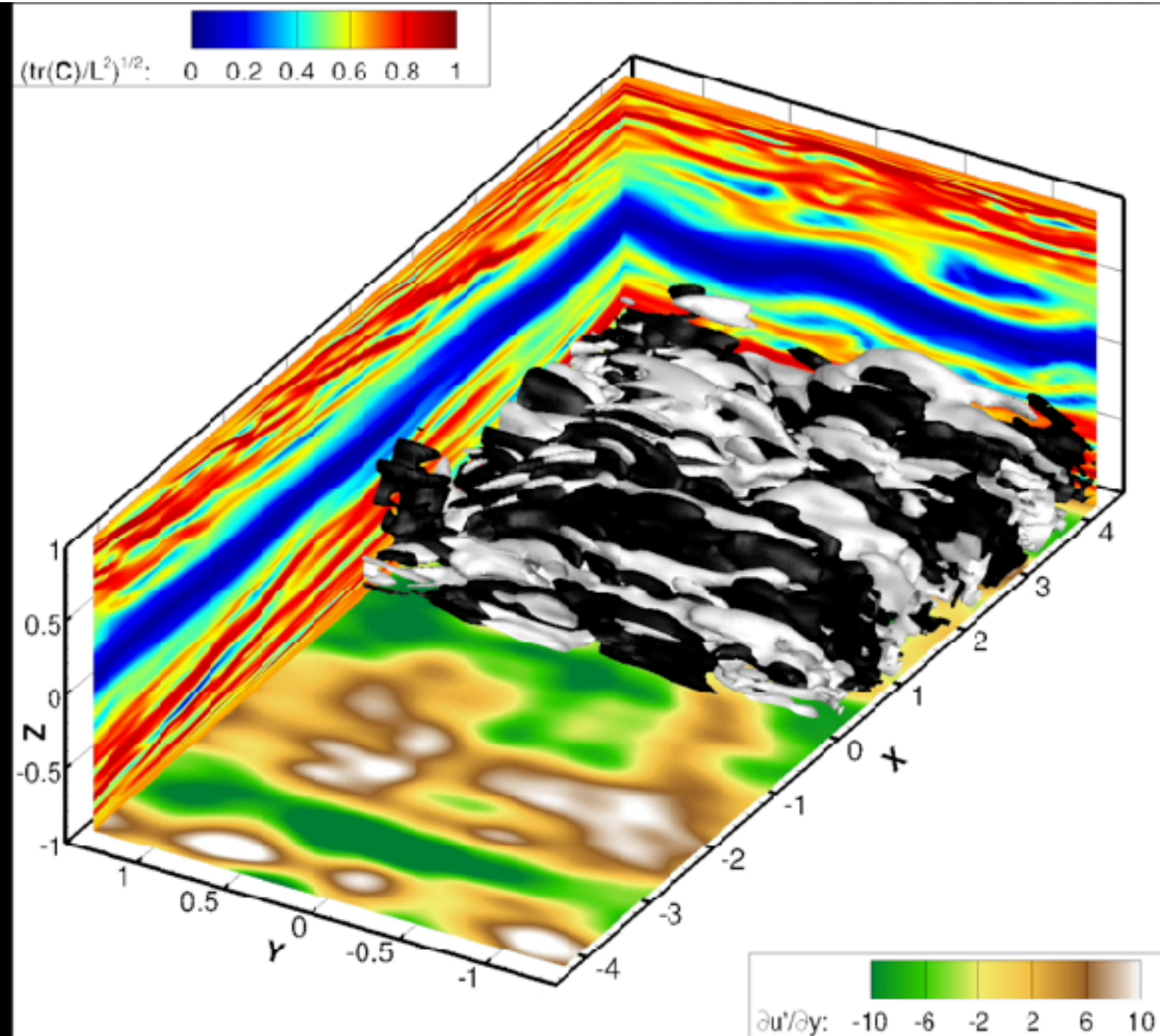
Grounds for Assumption II (MDR=EIT)

$$Re_\tau = 84.96, \beta = 0.97, L = 70.7, Wi_\tau = 40$$



Grounds for Assumption II (MDR=EIT)

$$Wi_{\tau} = 100$$



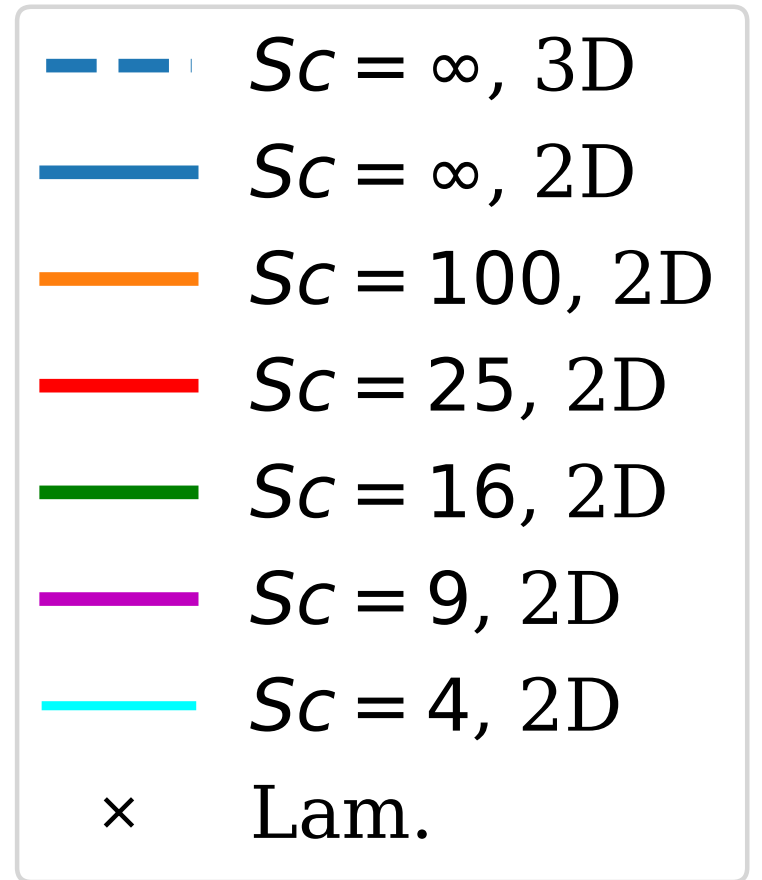
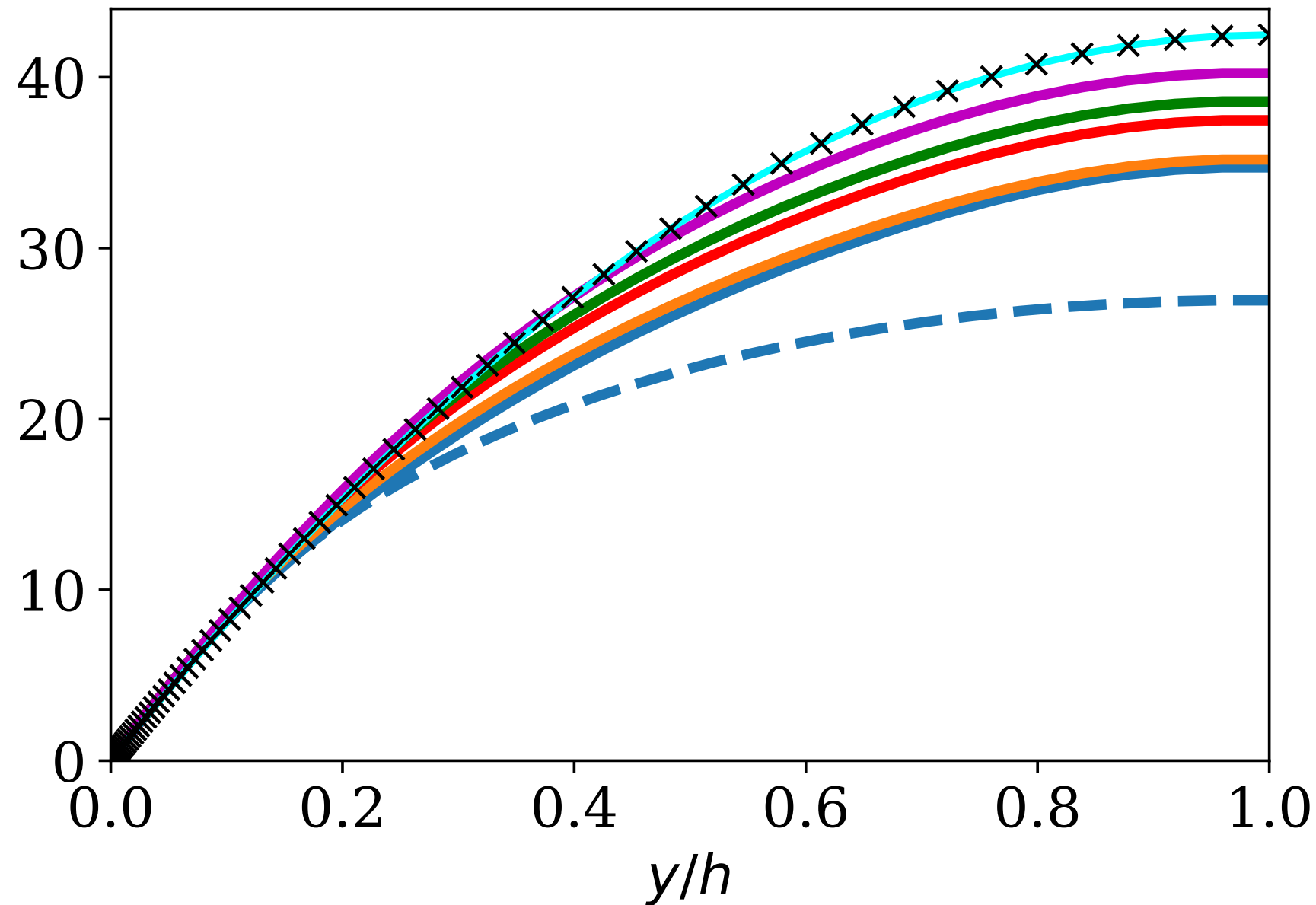
Effect of Schmidt Number in 2D simulation

$$Re_\tau = 84.96, \beta = 0.97, L = 70.7, Wi_\tau = 40$$

$$\eta_\theta = \frac{\eta_K}{\sqrt{Sc}}$$

Batchelor scale
(passive scalar)

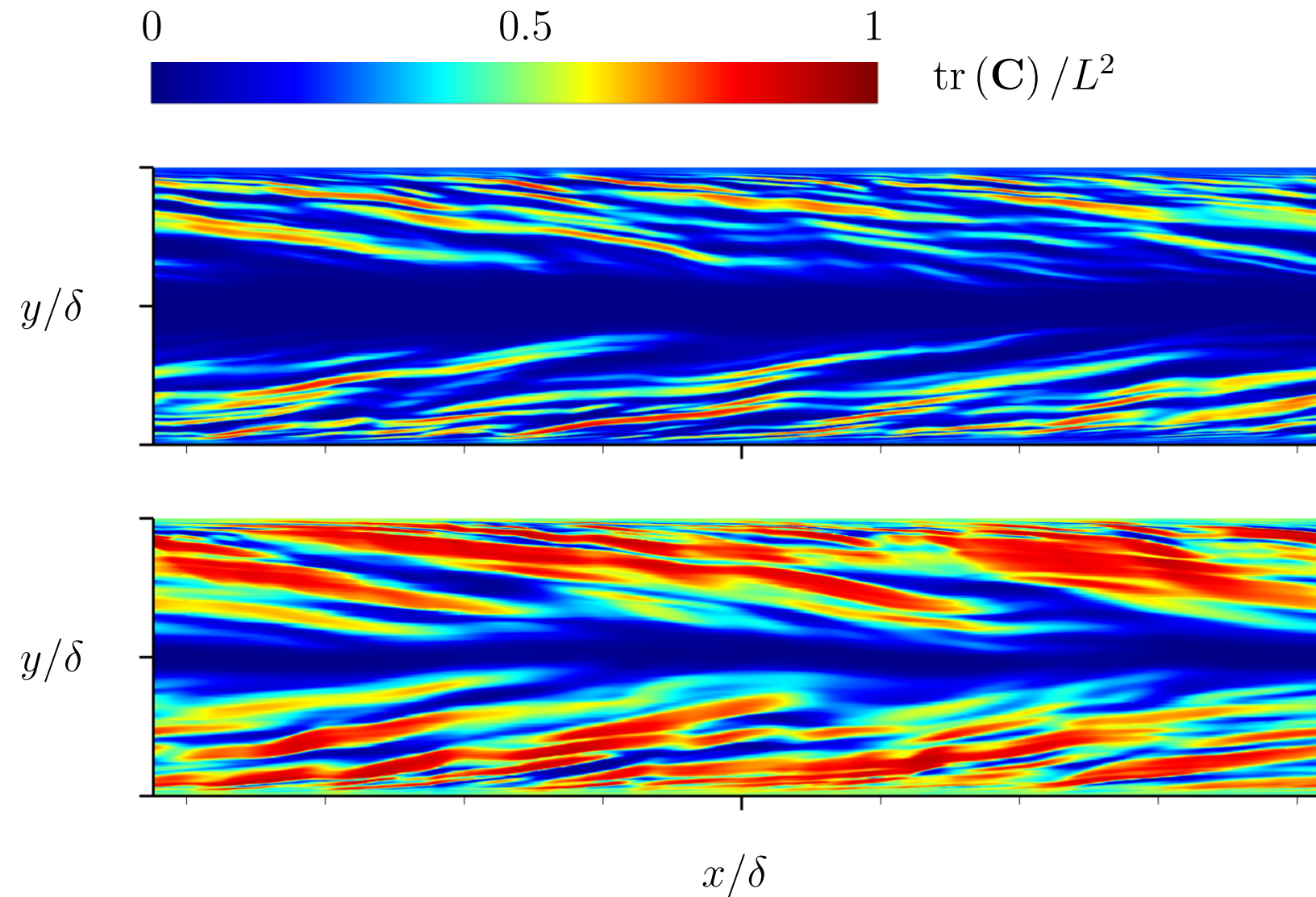
U



- EIT disappears for Schmidt number lower than 9

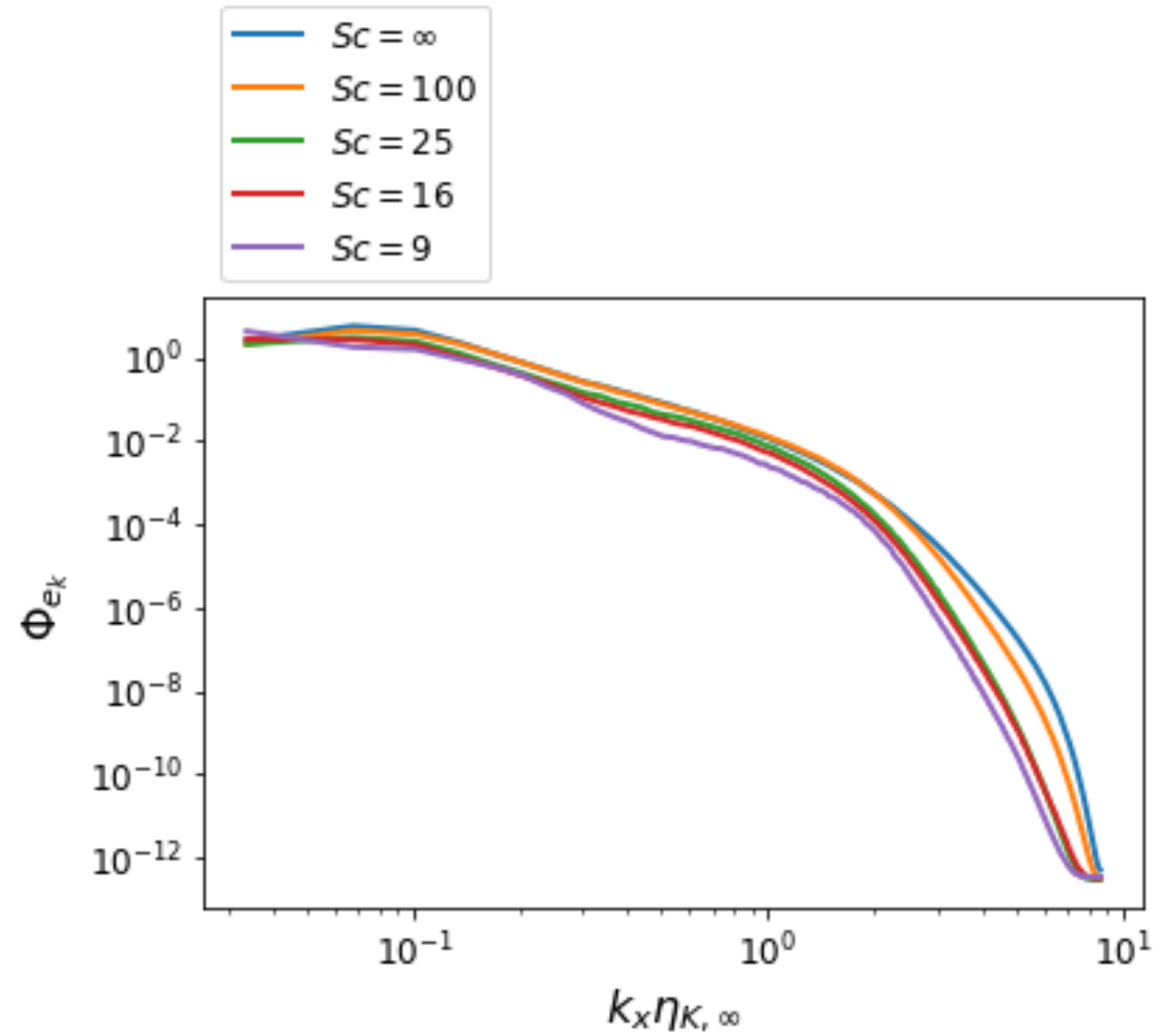
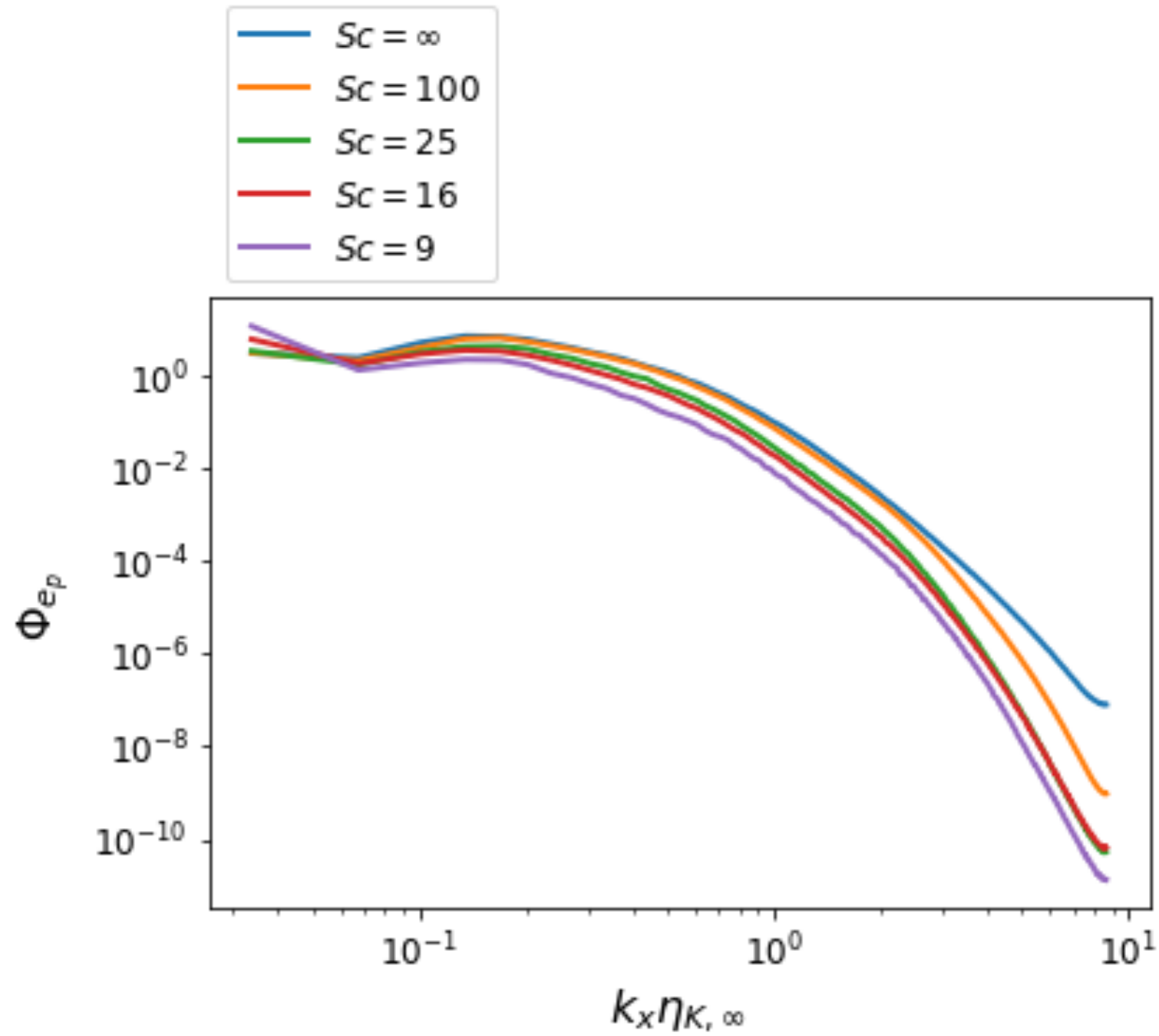
Visualization of Polymer Stretch in 2D Flows

$$Re_\tau = 84.96, \beta = 0.97, L = 70.7, Wi_\tau = 40$$
$$Wi_\tau = 100$$



- Typical sheet like structure

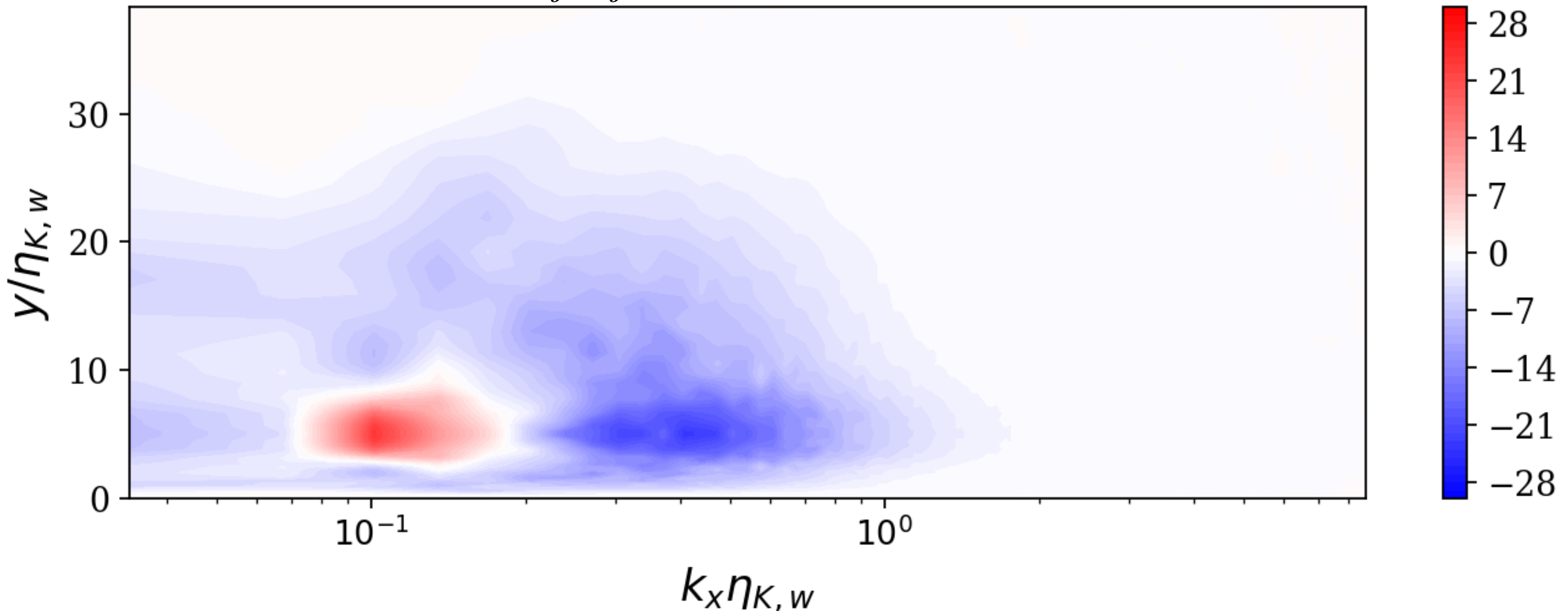
Spectra of Elastic Energy and TKE



Energy Transfer between Flow and Polymer in 2D

$$Re_\tau = 84.96, \beta = 0.97, L = 70.7, Wi_\tau = 40$$

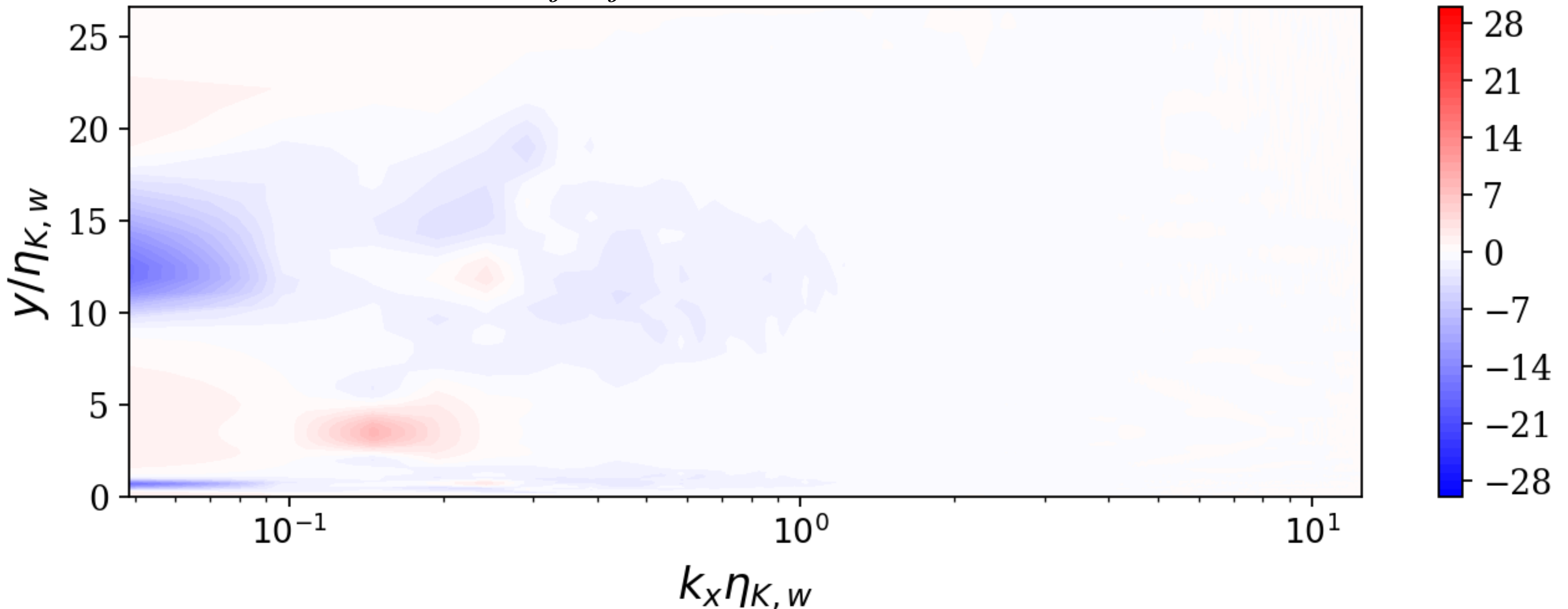
Co-spectra of $T_{ij}S_{ij}$ as function of distance from the wall



Energy Transfer between Flow and Polymer in 2D

$$Re_\tau = 84.96, \beta = 0.97, L = 70.7, Wi_\tau = 40$$

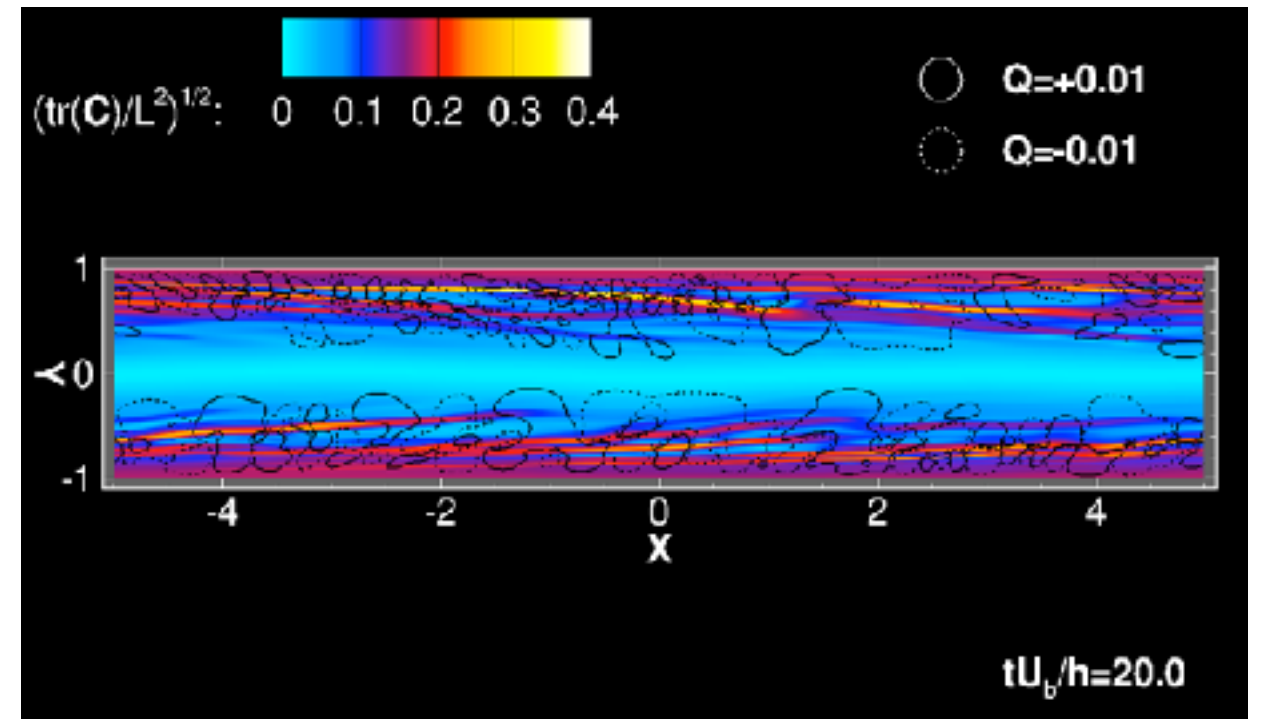
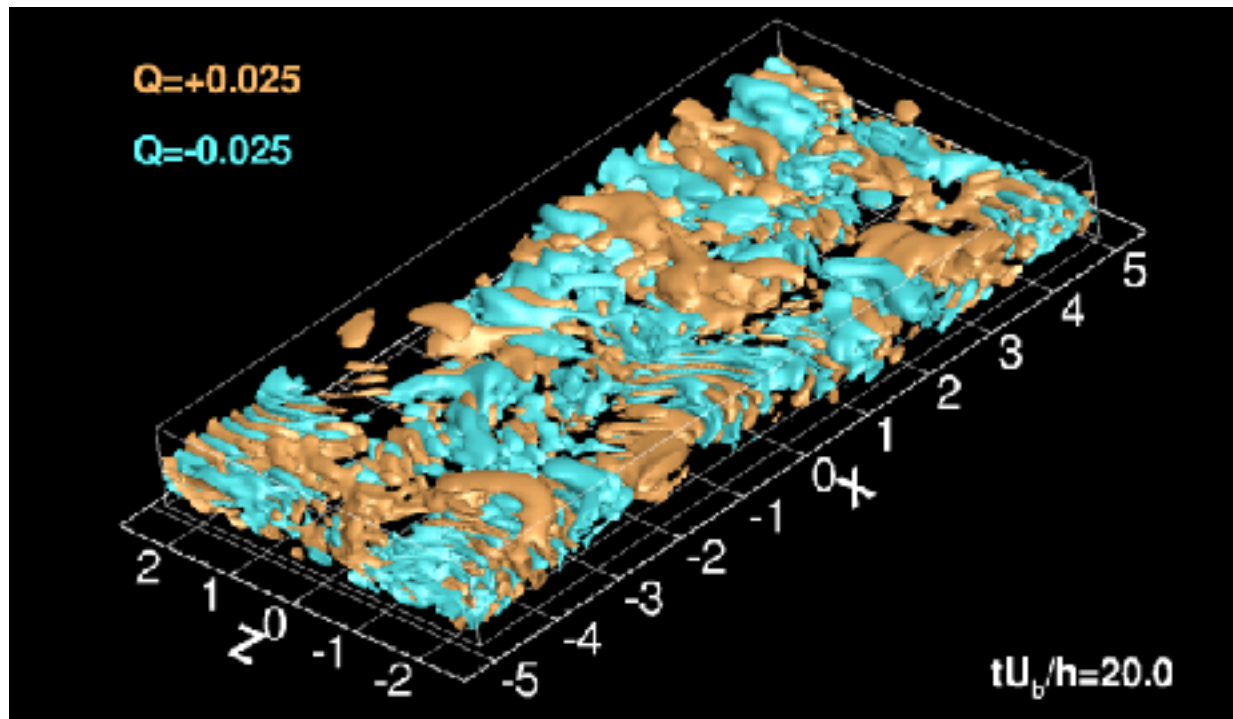
Co-spectra of $T_{ij}S_{ij}$ as function of distance from the wall



Conclusions

- **EIT is 2D**: For elastic solutions, given the right initial conditions, EIT will always exist
- **EIT is small scale**: The smaller the Reynolds number, the smaller the polymer dynamics' scale
- **EIT injects energy into the flow**: Without this backward cascade, EIT cannot exist
- **MDR = EIT**: For high elasticity, Newtonian vortices disappear
- **MDR is state of drag increase (compared to laminar)**

Mechanism of Elasto-Inertial Turbulence



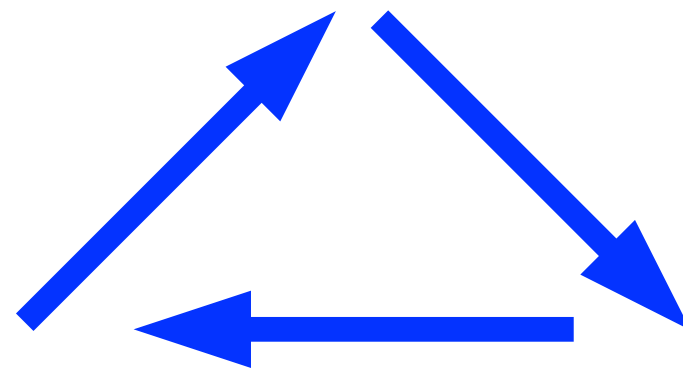
Mean shear +
 $\partial_t \mathbf{C} + (\mathbf{u} \cdot \nabla) \mathbf{C}$
 Formation of sheets of \mathbf{C}

$$\nabla^2 p = 2Q + \frac{1 - \beta}{Re} \nabla \cdot (\nabla \cdot \mathbf{T})$$

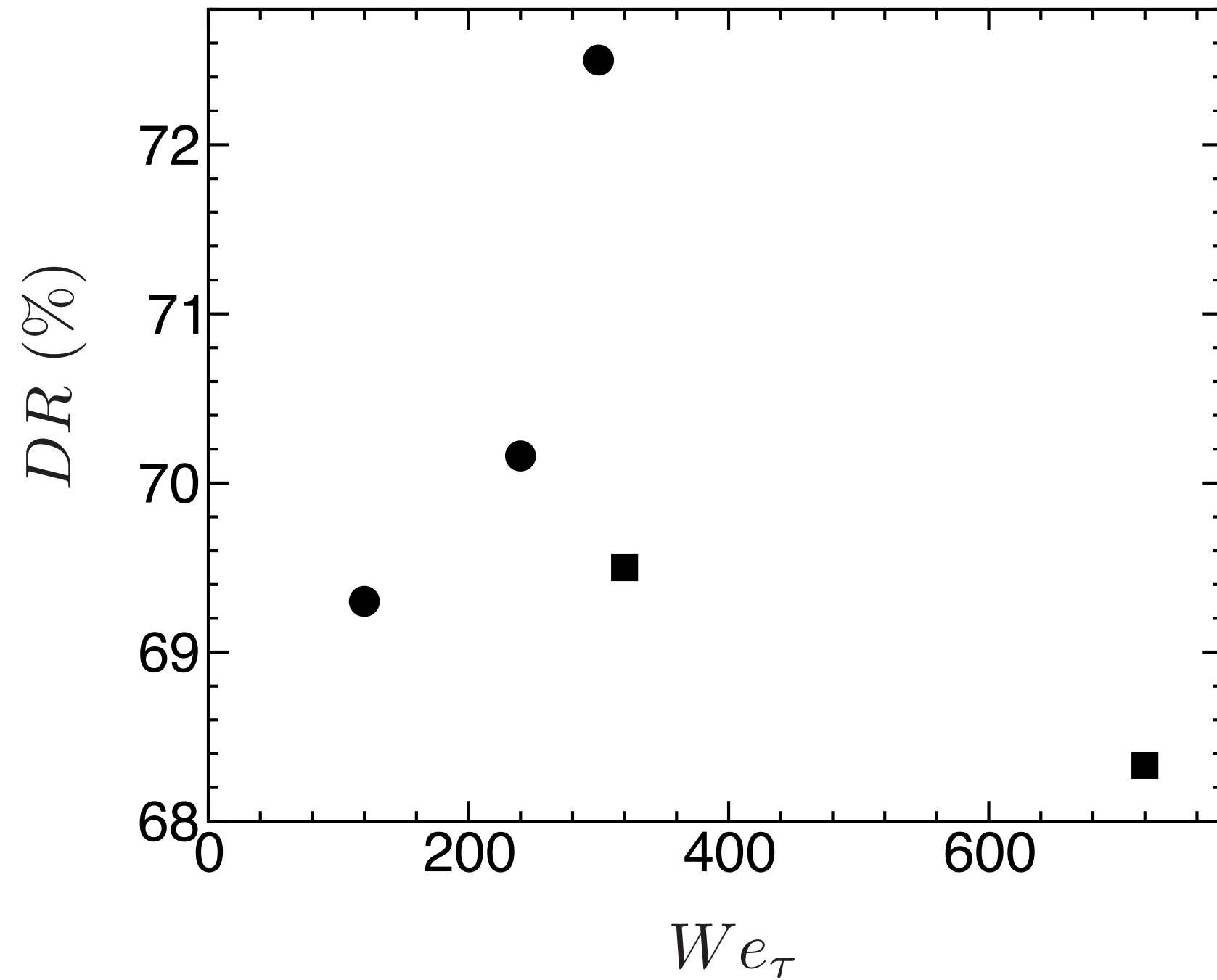
Excitation of extensional sheet flow and elliptical pressure redistribution of energy

$$\mathbf{C} \cdot (\nabla \mathbf{u}) + (\nabla \mathbf{u})^t \cdot \mathbf{C} - \mathbf{T}$$

Increase of extensional viscosity in sheets



$Re_b = 10000$. Effect of Weissenberg number



Overshoot of drag reduction (DR) Dubief, 2010

Flow topology

Deformation rate tensor

$$\mathbf{S} = \frac{1}{2} (\nabla \mathbf{u} + \nabla \mathbf{u}^t)$$

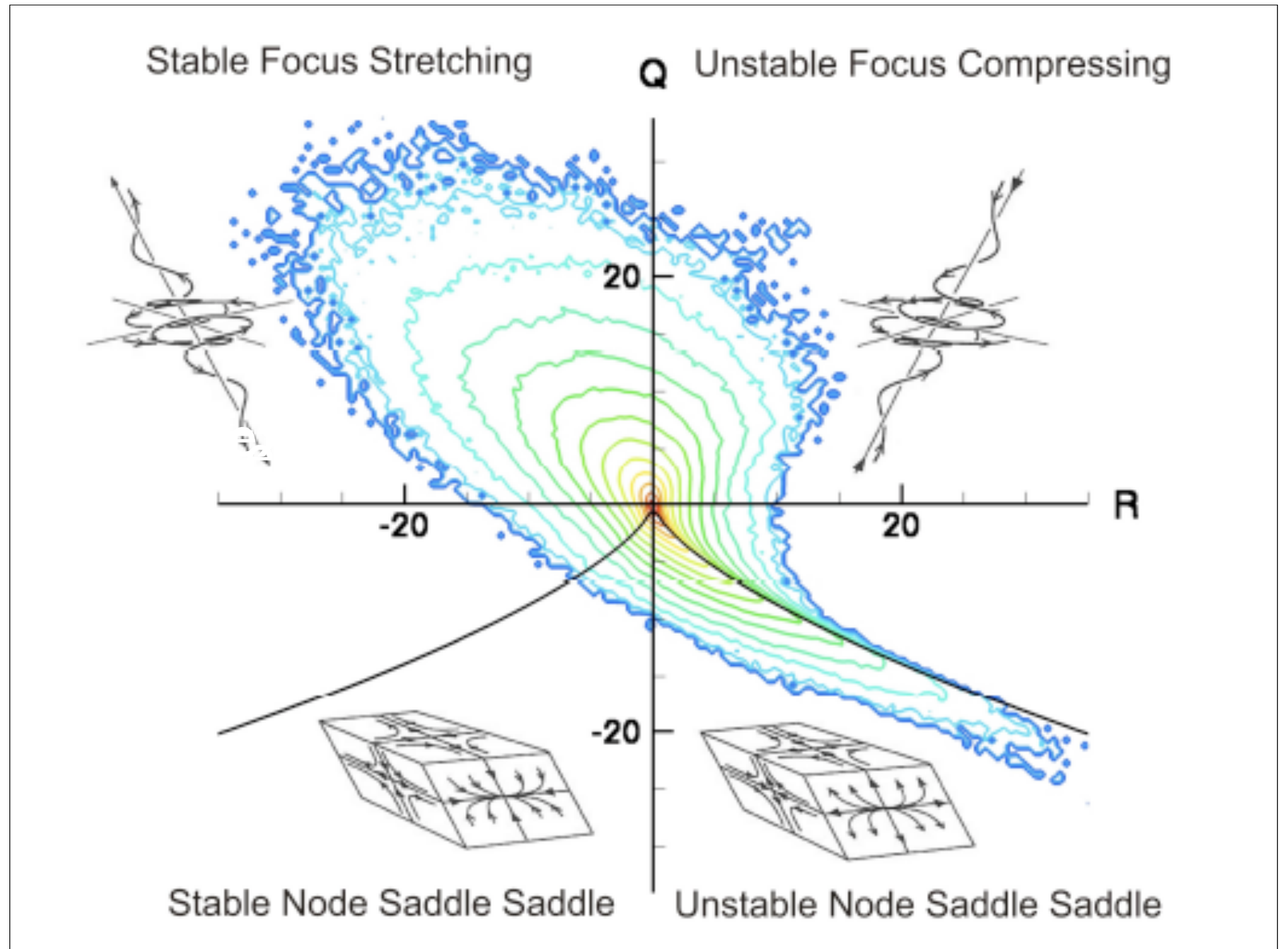
Rotation rate tensor

$$\mathbf{\Omega} = \frac{1}{2} (\nabla \mathbf{u} - \nabla \mathbf{u}^t)$$

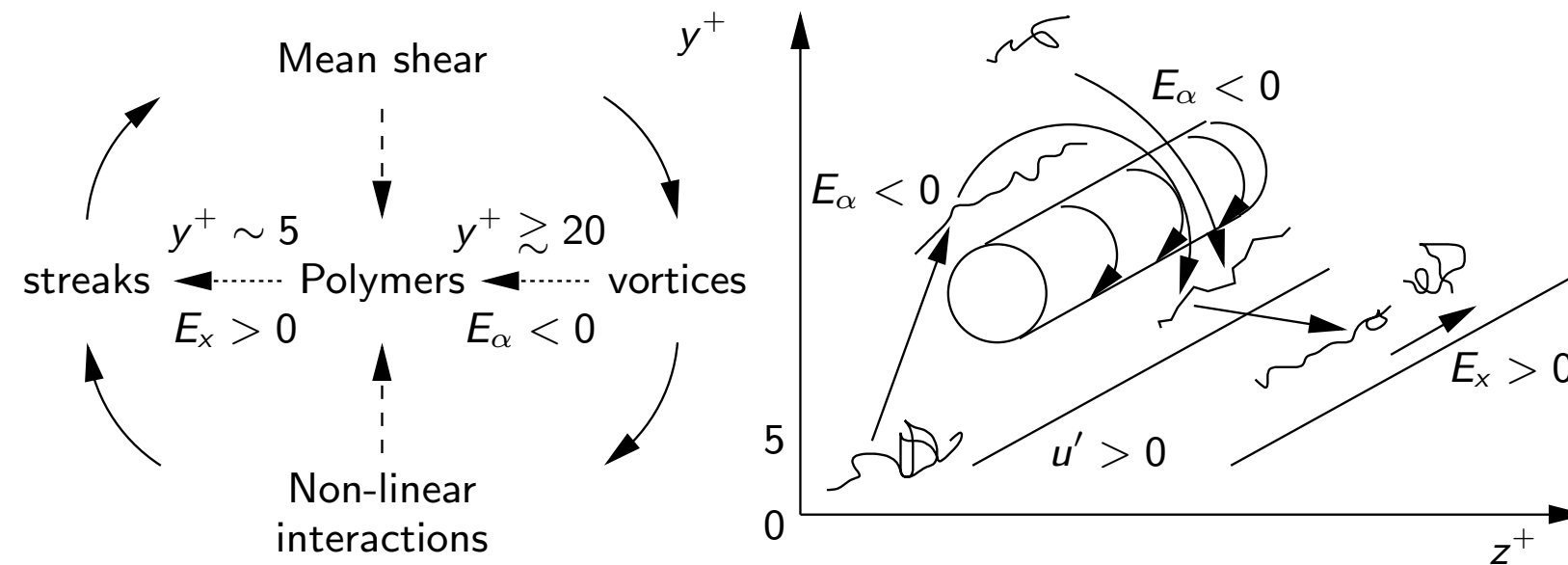
Second invariant of velocity gradient tensor

$$Q = \frac{1}{2} (\mathbf{\Omega}^2 - \mathbf{S}^2)$$

$Q > Q_{th} > 0$ = vortex identification method (Hunt et al, CTR 1998, Dubief & Delcayre, JoT 2000)



Mechanism of polymer drag reduction



$$\frac{1}{2} \frac{Du_i^2}{Dt} = \underbrace{u_i \partial_i p + u_i \frac{\beta}{Re} \partial_j \partial_j u_i}_{N_i} + \underbrace{u_i \frac{1-\beta}{Re} \partial_j \tau_{ij}}_{E_i} \quad \text{no summation on } i$$

$$\frac{Dk}{Dt} = N + E, \quad k = \frac{1}{2} u_j u_j, \quad E_\alpha = E_y \text{ or } E_z$$

N is the Newtonian contribution, E is the viscoelastic contribution

Schematic of elastic contribution to local turbulent kinetic energy

Dubief et al. JFM 2004, Terrapon et al. JFM 2004

Net effect: Polymers apply a negative torque on near-wall vortices by extending in regions of biaxial extensions created by the same vortices